

Stability of the body-centered-tetragonal phase of Fe at high pressure: Ground-state energies, phonon spectra, and molecular dynamics simulations

A. B. Belonoshko,^{1,2} E. I. Isaev,^{3,4} N. V. Skorodumova,³ and B. Johansson³

¹*Applied Materials Physics, Department of Materials Science and Engineering, The Royal Institute of Technology, SE-100 44 Stockholm, Sweden*

²*Condensed Matter Theory, AlbaNova University Center, Department of Physics, The Royal Institute of Technology, SE-106 91 Stockholm, Sweden*

³*Condensed Matter Theory Group, Department of Physics, Box 530, Uppsala University, SE-751 21 Uppsala, Sweden*

⁴*Theoretical Physics Department, Moscow State Institute of Steel and Alloys (Technological University), 4 Leninskii prospect, Moscow 119049, Russia*

(Received 21 May 2006; revised manuscript received 17 August 2006; published 4 December 2006)

It is well established that at a pressure of several megabars and low temperature Fe is stable in the hexagonal-close-packed (hcp) phase. However, there are indications that on heating a high-pressure hcp phase of Fe transforms to a less dense (open structure) phase. Two phases have been suggested as candidates for these high-temperature stable phases: namely, body-centered-cubic and body-centered-tetragonal (bct) phases. We performed first-principles molecular dynamics and phonon analysis of the bct Fe phase and demonstrated its dynamical instability. This allows us to dismiss the existence of the bct Fe phase under the high-pressure high-temperature conditions of the Earth's inner core.

DOI: [10.1103/PhysRevB.74.214102](https://doi.org/10.1103/PhysRevB.74.214102)

PACS number(s): 64.10.+h, 64.70.Dv, 71.15.Pd

I. INTRODUCTION

The iron phase diagram in a wide pressure range is of a considerable interest for modern technology and geophysics. Iron is certainly one of the most important materials at ambient conditions. Moreover, iron is thought to be a major (slightly alloyed by Ni and some light elements) component of the Earth core¹ where it is exposed to high pressure and temperature. The pressure-temperature range of the solid inner core (IC) is between 3.3 and 3.6 megabars (Ref. 2) and 4000 and 8000 K (Refs. 3–10). In the pressure range of the IC but at low temperatures Fe is known to be stable in the hexagonal-close-packed (hcp) structure.⁵ Interest in Fe phases alternative to hcp emerged when shock-wave experiments had demonstrated¹¹ (not unambiguously, though^{12–14}) that there was a solid-solid phase transition prior to melting at pressures above 2 Mbar and temperatures between 4000 and 5000 K. This interest was further supported by the demonstration that the body-centered-cubic (bcc) phase of iron could possess closer properties to those of the Earth's IC (Ref. 2) than the hcp phase.¹⁵ Moreover, it was demonstrated^{16,17} that in diamond anvil cell experiments there was a possibility to misinterpret an hcp-bcc transition as a melting. Therefore, the bcc phase of iron was under close consideration as a possible component of the Earth's IC.^{9,18} While one of the performed studies⁹ suggests that the bcc phase is stable at the regarded conditions, the other one¹⁸ suggests instead the stability of the hcp phase; however, free energies of bcc and hcp appear to be very close to each other. It was suggested¹⁹ that the bcc phase is unlikely to be stable in the Earth's core because it was found¹⁹ that the bcc iron phase becomes dynamically unstable at high pressure. As we now know, such a suggestion is not justified. At high temperature, the bcc phase becomes dynamically stable^{9,18} despite the instability at $T=0$ K. We notice that the bcc phase is not the only iron structure which might have been found in the

shockwave experiments.¹¹ Another phase, which is slightly lower in energy at $T=0$ K and high pressure, is the body-centered-tetragonal (bct) phase.²⁰ As the bct phase is lower in energy than bcc at pressures relevant to the Earth's IC one might assume that the former phase can be more stable at the IC conditions than the latter one. Moreover, along the Bain path, the energy of the body-centered phase exhibits a minimum at the bct configuration ($c \neq a$), while the energy of the bcc phase is at a maximum.²⁰ This unambiguously tells us that the bcc phase is dynamically unstable, while the bct phase might be dynamically stable at $T=0$ K. Therefore, there is a need to study a possible stability of this phase at high pressure. The bct phase has already been investigated theoretically and based on the analysis of the elastic moduli it has been shown to stabilize at pressures above 180 GPa.²¹ However, the validity of the applied method used to calculate the elastic constants²¹ was objected to;²² therefore, these results remain unconfirmed.

In this paper we theoretically investigate the stability of bct Fe at low and high temperatures and at pressures relevant to the IC. The paper is organized as follows. First, we describe the methods used to perform the calculations of the ground-state energies, phonon spectra, and molecular dynamics simulations for both the bcc and bct phases (Sec. II). Second, we describe the obtained results and discuss them in the perspective of their importance for Earth science (Sec. III). In the Conclusions section we outline the future directions of studies on stability of high-temperature phases, unstable at zero and/or low temperatures.

II. METHODS

A. Total energy and phonon calculations

The calculations of the total energies were done by the projector augmented-wave (PAW) method²³ [as implemented

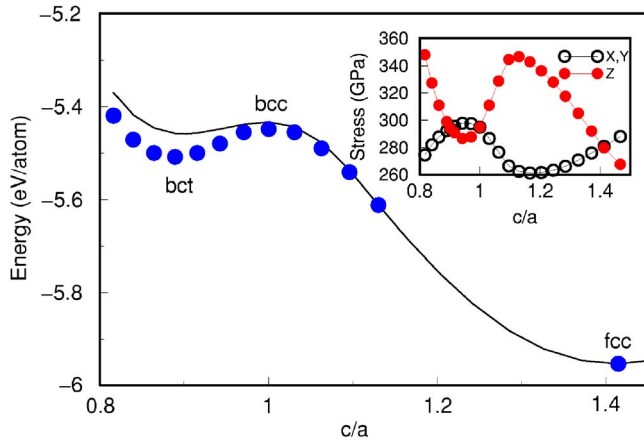


FIG. 1. (Color online) The calculated energy of iron phases along the Bain path at the volume $6.91 \text{ \AA}^3/\text{atom}$. The solid curve shows the results of non-magnetic calculations, whereas solid circles represent the data obtained from spin-polarized calculations. The insert shows stresses along X , Y , and Z direction depending on the c/a ratio.

in VASP (Ref. 24)] based on density functional theory (DFT) within the generalized gradient approximation (GGA) using the Perdew-Wang parametrization.²⁵ The calculations were performed with a cutoff energy of 27 Ry, treating $3p$, $3d$, and $4s$ orbitals as Fe valence states. The $16 \times 16 \times 16$ Monkhorst-Pack k -point mesh²⁶ was used. The Brillouin-zone (BZ) integration was done by the linear tetrahedral method with Blöchl corrections.²⁷ Both spin-polarized and nonpolarized calculations were carried out for the iron structures along the Bain path.

In order to analyze the dynamic stability of bct Fe we performed phonon calculations using the Quantum Espresso package²⁸ based on density functional perturbation theory²⁹ (DFPT) and *ab initio* pseudopotential approximation to the electron-ion interaction. In our phonon studies we used an ultrasoft pseudopotential³⁰ generated using three Bessel functions, as proposed by Rabe *et al.*³¹ and generalized-gradient corrections to the exchange-correlation functional according to Perdew, Burke, and Ernzerhof.³² The electron wave function in a periodic crystal was presented as a sum of plane waves with kinetic energy up to 40 Ry, and plane waves with energy up to 480 Ry were used to describe the augmented charge. In addition, we tested phonon frequencies for the high-symmetry X point in the Brillouin zone using the cutoff energies 60 Ry and 720 Ry, and found them to be converged with an accuracy of 0.3 THz or 10%. Integration over the BZ was performed using a $18 \times 18 \times 18$ k -point mesh and a special-points technique²⁶ with broadening $\sigma=0.02$ Ry according to the Marzari-Vanderbilt “cold” smearing method.³³ Phonon dispersion curves along high-symmetry directions were calculated using the force constants $C_{ij}^{\alpha\beta}(R)$, obtained by means of fast Fourier transformation of 13 dynamical matrices $C_{ij}^{\alpha\beta}(q)$, where i and j are atomic indexes and α and β are polarization directions. The self-consistent and phonon calculations were converged within 10^{-10} Ry and 10^{-14} Ry, respectively.

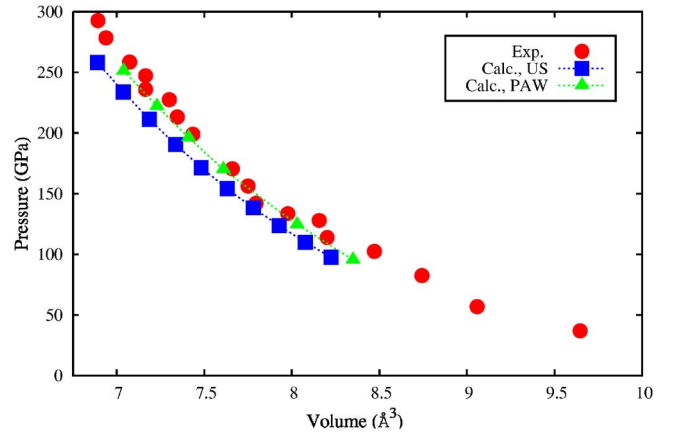


FIG. 2. (Color online) Equation of state for hcp Fe. Solid circles refer to experimental values (Ref. 5). Solid squares and triangles stand for our calculated pressure for a given volume by the pseudopotential and all-electron PAW methods, respectively. The c/a for hcp Fe was suggested to be pressure independent (see text), and in our calculations we used $c/a=1.588$.

B. Molecular dynamics simulations

To check if the bct phase can be stabilized by high temperature, similar to the bcc phase^{9,18} (which is dynamically unstable at low T and high P , but becomes dynamically stable on increasing T) we employed the most straightforward method of molecular dynamics (MD).

We performed *ab initio* molecular dynamics (AIMD) simulations of the iron bcc and bct structures in NVT ensemble (N , number of atoms; V , volume; T , temperature). The calculations of energies were done as the described-above PAW calculations. Since our supercells were large ($N=128$), the calculations were performed with the Γ point only. The computational cells for the calculations of bct and bcc supercells were obtained as $4 \times 4 \times 4$ bcc and bct unit cells, correspondingly. Since both the bcc and bct unit cells contain two atoms, the number of atoms was 128 in both AIMD runs. The temperature and volume were chosen to be within the likely range of the Earth’s IC—that is, 6000 K and $6.91 \text{ \AA}^3/\text{atom}$. Simulated systems were coupled to the Nosé thermostat with the mass to provide a period of oscillation of about 40 time steps. The time step was equal to 1 fsec. About 2000 time steps were performed in both AIMD runs. In AIMD, the c/a ratio of the bct phase was chosen equal to that corresponding to the energy minimum (Fig. 1).

III. RESULTS AND DISCUSSION

According to our as well as numerous previous results the bcc structure is the stable phase of iron at zero temperature and pressure. As pressure increases up to about 200 GPa, bcc becomes unstable with respect to a tetragonal distortion, which results in the appearance of a local minimum in the total energy dependence versus c/a ratio (Fig. 1). Figure 1 shows the dependence of the total energy on c/a ratio for the volume $6.91 \text{ \AA}^3/\text{atom}$ corresponding to ~ 295 GPa. Thus at high pressures bct Fe has lower energy than bcc Fe, although the energy of bct is significantly higher than those of the

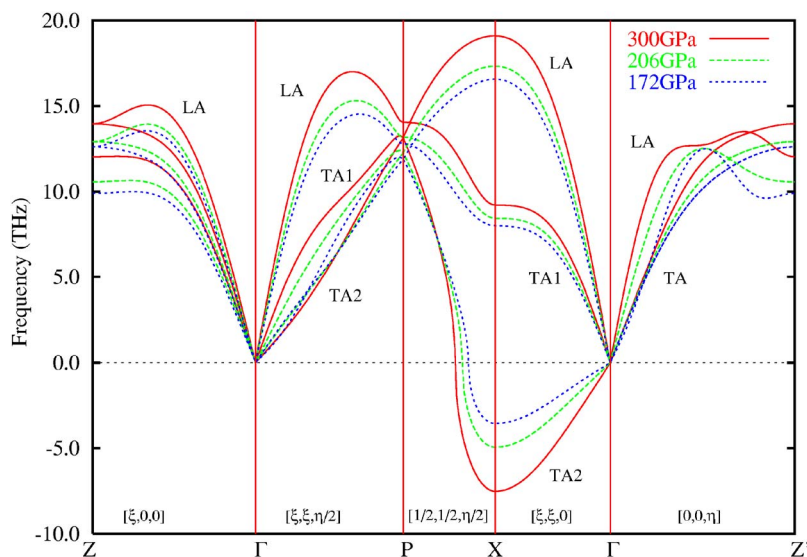


FIG. 3. (Color online) Phonon dispersion relations in bct Fe ($c/a=0.887$) as a function of pressure. Solid curves show phonon modes at 300 GPa, long-dashed curves are phonon dispersion curves at 206 GPa, and phonons at 300 GPa are shown by dotted curves. LA and TA stand for the longitudinal and transversal acoustic modes, respectively. Soft TA2 mode along $[\xi, \xi, 0]$ induces the dynamical instability of bct Fe. Notations for high-symmetry directions are given in Cartesian coordinates.

close-packed structures, in particular the fcc structure (Fig. 1). The obtained c/a ratio for the bct phase, 0.887, is in good agreement with previously reported values.²⁰ At a tetragonal distortion of the bcc phase stresses along x , y , and z directions deviate from each other but they become equal again for $c/a=0.887$, corresponding to the local energy minimum for the tetragonal phase, and for $c/a=1.414$, corresponding to the fcc phase. Interestingly, the uniform stresses are very similar for bcc and bct. Different from close-packed structures of iron the bct phase sustains a substantial magnetic moment even at 300 GPa ($\sim 0.7 \mu\text{B}/\text{atom}$), similar to the bcc phase.

To investigate the stability of the found bct phase we performed phonon calculations in the framework of the DFPT (see above). As far as we used an ultrasoft pseudopotential in the Quantum Espresso code, we carried out transferability tests in order to be sure that it describes properly ground-state parameters, as well as the Fe equation of state (EOS) at high pressures. The calculated ground-state parameters of bcc Fe, the lattice parameter $a=2.86 \text{ \AA}$ and bulk modulus $B=150 \text{ GPa}$, agree well with the theoretical and experimental values 2.87 \AA and $B=168 \text{ GPa}$.³⁴ Then we optimized the c/a ratio for hcp Fe in the low- (20 GPa) and high-

(210 GPa) pressure limit and found it to be slightly lower (1.582 for 20 GPa and 1.589 for $P=210 \text{ GPa}$) than the experimental 1.603,³⁴ which is believed to be almost pressure independent. A similar c/a value, 1.585, was obtained in Ref. 20 using the full-potential linear muffin-tin orbital (LMTO) method. The calculated EOS for hcp Fe is shown in Fig. 2 which reveals good agreement between theoretical and experimental EOS. We have also calculated the hcp equation of state by applying the PAW (see above) method and following the same as described above procedure. The results are presented in Fig. 2. The PAW results match the experiment better than those obtained by the pseudopotential method. We note that this is not critical, since both methods provide the data reasonably close to the experimental set (Fig. 2). Besides, the calculated pressure, 298 GPa, for bct Fe with atomic volume 6.91 \AA^3 is in remarkable agreement with pressure, 295 GPa, obtained in this work using PAW pseudopotential with 14 valence electrons. Note that the phonon spectrum of bcc Fe calculated before³⁵ using the pseudopotential is in quite good agreement with results of inelastic neutron scattering experiments.

Our calculated phonon dispersion curves for bct Fe with $c/a=0.887$ as a function of pressure are presented in Fig. 3.

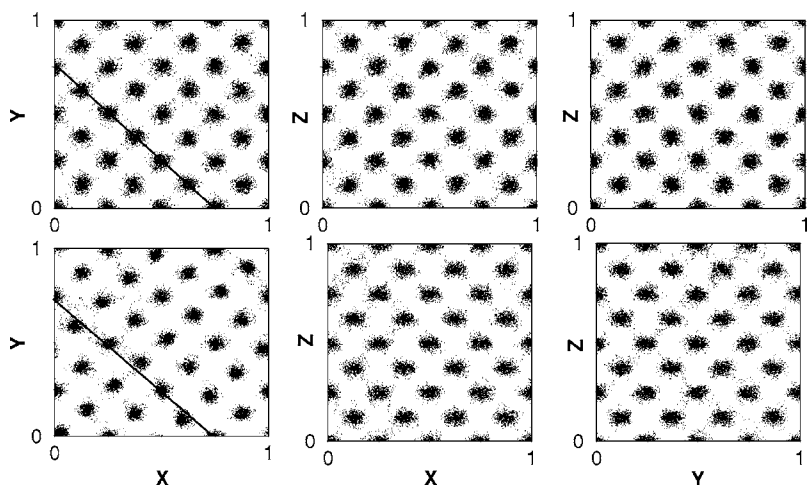


FIG. 4. Three projections (XY, XZ, and YZ, from left to right) of every 12th configuration obtained during AIMD for the bcc (upper row) and bct (lower row) phases. The atoms are plotted by small circles. Since there are about 200 points for each atom, the atomic positions form a “cloud.” Note also that while atoms of the bcc phase belong to the 110 plane (straight line in the upper leftmost picture), the corresponding atoms in the bct phase are distorted and do not belong to the same plane (the planes are shown by straight lines).

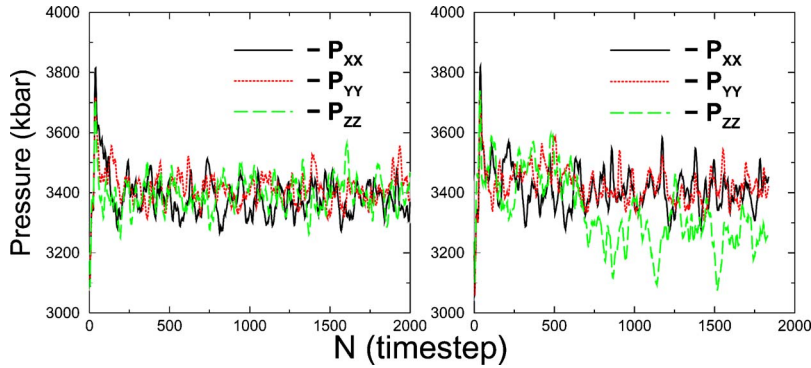


FIG. 5. (Color online) Time dependence of pressure components during AIMD simulations of bcc (left) and bct (right) phases.

The studied pressure range covers the predicted interval of bct Fe stability³⁶ (Fig. 3). We considered three pressures (P): namely, $P=170$, 206 , and 300 GPa. At $P=170$ GPa the shear modulus $C'=(C_{11}-C_{12})/2$, where C_{11} and C_{12} are elastic constants, is negative;³⁶ therefore, bct Fe is mechanically unstable. At $P=206$ GPa, C' becomes positive,³⁶ indicating a possible mechanical stability of bct Fe. The third $P=300$ GPa is close to IC conditions and the occurrence (stabilization) of the bct phase might be expected. Under high pressure a “hardening” (i.e., increase in energy) of the phonon spectra along the ΓZ and $\Gamma Z'$ directions is observed. Besides, near $\frac{1}{2}\Gamma Z'$ a softening of the longitudinal acoustic (LA) mode occurs. At the $Z(100)$ point the threefold degeneracy, characteristic for the bcc lattice at the $H(100)$ point, is left due to nonuniform compression along z axis. In the ΓP direction, LA and transversal acoustic (TA1) modes also become harder, but the TA2 mode somewhat softens near the $\frac{1}{3}\Gamma P$ point. An interesting feature in the phonon spectrum of bct Fe is the appearance of a soft TA2 mode at the X point, which means that the conclusion on the stability of the bct Fe phase³⁶ is not correct. As pressure increases the TA2 mode is enhanced and, therefore, promotes the dynamical instability of bct Fe. Recently, it has been shown²² that the description of the elastic constants in bct Fe, provided by Ma and co-workers,^{36,37} might be not correct due to the definition of elastic constants as the second derivative of the Gibbs energy, but not the total energy. Indeed, elastic moduli for Fe and Re obtained using volume-conserving strains agreed well with experimental data in a wide pressure range³⁸ without any pressure correction. High-pressure elastic moduli obtained using volume-not-conserving strains might result in positive C' for bct Fe. In fact, C' , calculated by means of derivatives of the TA2 mode, should be negative (see Fig. 3), indicating mechanic instability of bct Fe at these pressure ranges.

We know that dynamic instability of a phase at $T=0$ K not necessary means its instability at high T . For example, the bcc Fe phase, being dynamically unstable at high pressure and $T=0$ K, becomes dynamically stable at high T according to virtually any kind of model.^{7–9,15,18} Therefore, to find out if the bct phase, being unstable at low T , becomes stable at high T , we performed the AIMD simulations as described above (see Methods). Indeed, in accordance with the previous results,^{9,18} we see the dynamical stability of the bcc Fe phase. The bcc structure (Fig. 4) remains intact while atoms vibrate around their equilibrium positions. The three

trace components of the pressure tensor P_{xx} , P_{yy} , and P_{zz} also fluctuate around the same average value (Fig. 5). This indicates that the bcc Fe phase is dynamically stable at a pressure of about 340 GPa and temperature of 6000 K. In contrast, the bct Fe phase behaves quite differently. The bct structure (Fig. 4) is distorted, with the atoms sliding out of the crystal planes. Note that the XY plane becomes the most distorted (Fig. 4) in agreement with the corresponding instability trend obtained by phonon calculations (Fig. 3). The trace of the pressure tensor (Fig. 5) is split with the P_{zz} very different from P_{xx} and P_{yy} . This behavior of the pressure components indicates that the computational cell would change its shape if this would have been allowed. The result of our AIMD simulations indicate that the bct phase is not stabilized by high T , unlike the bcc phase, and therefore should not be considered as a possible stable phase in the Earth inner core.

IV. CONCLUSIONS

For quite some time consideration of structures other than close-packed ones was discouraged by the observation of their dynamical instability at high pressure. We know now that the dynamical instability at low T might reverse to a stability at high T . We do not fully understand yet the mechanism behind such a reversal. Therefore, it is even more important to approach the consideration of stability as rigorously as possible. Since the bct phase is unlikely to be stable under the conditions of the Earth’s inner core, the only alternative is the bcc phase. The bcc phase, being dynamically stable, has yet to be experimentally demonstrated to be stable or unstable thermodynamically.

ACKNOWLEDGMENTS

Computations were performed using the facilities of the National Supercomputer Center in Linköping and the Parallel Computer Center in Stockholm. We also wish to thank the Swedish Research Council (VR) and the Swedish Foundation for Strategic Research (SSF) for financial support. E.I.I. thanks the Russian Foundation for Basic Researches (RFBR, Grants No. 04-02-16823 and No. 06-02-17542), the Netherlands Organization for Scientific Researches (NWO, Grant No. 047.016.005), and the Royal Swedish Academy of Sciences (KVA) for financial support.

- ¹F. Birch, *J. Geophys. Res.* **57**, 227 (1952).
- ²A. M. Dziewonski and D. L. Anderson, *Phys. Earth Planet. Inter.* **25**, 297 (1981).
- ³R. Boehler, *Nature (London)* **363**, 534 (1993).
- ⁴C. S. Yoo, J. Akella, A. J. Campbell, H. K. Mao, and R. J. Hemley, *Science* **270**, 1473 (1995).
- ⁵R. J. Hemley and H. K. Mao, *Int. Geol. Rev.* **43**, 1 (2001).
- ⁶Y. Ma *et al.*, *Phys. Earth Planet. Inter.* **143-144**, 455 (2004).
- ⁷A. B. Belonoshko and R. Ahuja, *Phys. Earth Planet. Inter.* **102**, 171 (1997).
- ⁸A. B. Belonoshko, R. Ahuja, and B. Johansson, *Phys. Rev. Lett.* **84**, 3638 (2000).
- ⁹A. B. Belonoshko, R. Ahuja, and B. Johansson, *Nature (London)* **424**, 1032 (2003).
- ¹⁰D. Alfé, M. J. Gillan, and G. D. Price, *Nature (London)* **401**, 462 (1999).
- ¹¹J. M. Brown and R. G. McQueen, *J. Geophys. Res.* **91**, 7485 (1986).
- ¹²A. B. Belonoshko, *Science* **275**, 955 (1997); **278**, 1475 (1997).
- ¹³J. H. Nguyen and N. C. Holmes, *EOS Trans. Am. Geophys. Union* **79**, F846 (1998).
- ¹⁴J. H. Nguyen and N. C. Holmes, *Nature (London)* **427**, 339 (2004).
- ¹⁵M. Matsui and O. L. Anderson, *Phys. Earth Planet. Inter.* **103**, 55 (1997).
- ¹⁶A. B. Belonoshko, R. Ahuja, and B. Johansson, *Phys. Rev. Lett.* **87**, 165505 (2001); **89**, 119602 (2002); A. B. Belonoshko, O. LeBacq, R. Ahuja, and B. Johansson, *J. Chem. Phys.* **117**, 7233 (2002).
- ¹⁷A. B. Belonoshko, S. Davis, A. Rosengren, R. Ahuja, B. Johansson, S. I. Simak, L. Burakovsky, and D. L. Preston, *Phys. Rev. B* **74**, 054114 (2006).
- ¹⁸L. Vocadlo *et al.*, *Nature (London)* **424**, 536 (2003).
- ¹⁹D. M. Sherman, *AIP Conf. Proc. in High-Pressure Science and Technology—1993*, edited by S. C. Schmidt, J. W. Shaner, G. A. Samara, and M. Riss (AIP, New York, 1994), p. 895.
- ²⁰P. Söderlind, J. A. Moriarty, and J. M. Wills, *Phys. Rev. B* **53**, 14063 (1996).
- ²¹P. M. Marcus, H. Ma, and S. L. Qiu, *J. Phys.: Condens. Matter* **14**, L525 (2002).
- ²²G. Steinle-Neumann and R. E. Cohen, *J. Phys.: Condens. Matter* **16**, 8783 (2004); P. M. Marcus and S. L. Qiu, *ibid.* **16**, 8787 (2004).
- ²³P. E. Blöchl, *Phys. Rev. B* **50**, 17953 (1994).
- ²⁴G. Kresse and J. Furthmüller, *Comput. Mater. Sci.* **6**, 15 (1996); *Phys. Rev. B* **54**, 11169 (1996); G. Kresse and D. Joubert, *ibid.* **59**, 1758 (1999).
- ²⁵J. P. Perdew, J. A. Chevary, S. H. Vosko, K. A. Jackson, M. R. Pederson, D. J. Singh, and C. Fiolhais, *Phys. Rev. B* **46**, 6671 (1992).
- ²⁶H. J. Monkhorst and J. D. Pack, *Phys. Rev. B* **13**, 5188 (1976).
- ²⁷P. E. Blöchl, O. Jepsen, and O. K. Andersen, *Phys. Rev. B* **49**, 16223 (1994).
- ²⁸S. Baroni, A. Dal Corso, S. de Gironcoli, P. Giannozzi, C. Cavazzoni, G. Ballabio, S. Scandolo, G. Chiarotti, P. Focher, A. Pasquarello, K. Laasonen, A. Trave, R. Car, N. Marzari, and A. Kokalj, <http://www.pwscf.org/>
- ²⁹N. E. Zein, *Fiz. Tverd. Tela (Leningrad)* **26**, 3024 (1984) [*Sov. Phys. Tech. Phys.* **26**, 1825 (1984)]; S. Baroni, S. De Gironcoli, A. Dal Corso, and P. Giannozzi, *Rev. Mod. Phys.* **73**, 515 (2001).
- ³⁰The pseudopotential was originally generated by A. Dal Corso, for details see <http://www.pwscf.org/pseudo.htm/>
- ³¹A. M. Rappe, K. M. Rabe, E. Kaxiras, and J. D. Joannopoulos, *Phys. Rev. B* **41**, 1227 (1990).
- ³²J. P. Perdew, K. Burke, and M. Ernzerhof, *Phys. Rev. Lett.* **77**, 3685 (1996).
- ³³N. Marzari, D. Vanderbilt, A. De Vita, and M. C. Payne, *Phys. Rev. Lett.* **82**, 3296 (1999).
- ³⁴H.-K. Mao, W. A. Bassett, and T. Takahashi, *J. Appl. Phys.* **38**, 272 (1967).
- ³⁵A. Dal Corso and S. de Gironcoli, *Phys. Rev. B* **62**, 273 (2000).
- ³⁶H. Ma, S. L. Qiu, and P. M. Marcus, *Phys. Rev. B* **66**, 024113 (2002).
- ³⁷P. M. Marcus, H. Ma, and S. L. Qiu, *J. Phys.: Condens. Matter* **14**, L525 (2002).
- ³⁸G. Steinle-Neumann, L. Stixrude, and R. E. Cohen, *Phys. Rev. B* **60**, 791 (1999).